AIAA 81-0620R

Vibration of Prestressed Periodic Lattice Structures

Melvin S. Anderson*
NASA Langley Research Center, Hampton, Va.

Equations are developed for vibration of general lattice structures that have repetitive geometry. The method of solution is an extension of a previous paper on the buckling of similar structures. The theory is based on representing each member of the structure with the exact dynamic stiffness matrix and taking advantage of the repetitive geometry to obtain an eigenvalue problem involving the degrees-of-freedom at a single node in the lattice. Results are given for shell- and beam-like lattice structures and for rings stiffened with tension cables and a central mast. The variation of frequency with external loading and the effect of local member vibration on overall modes is shown.

Nomenclature

A = cross-sectional area of member
B = extensional stiffness of shell wall [$E_s t/(1-\nu^2)$ for isotropic shell wall]
C = concentrated mass at joint
C_j = joint mass moment of inertia about x_j axis
d_j, e_j = parameters from beam-differential equation defined in Eq. (A3)
E = Young's modulus
E_s = Young's modulus of shell wall
f = frequency
f_{ij} = dynamic stiffness coefficients [see Eq. (A3)]
F_j = force vector at node j [see Eq. (1)]
g^2 = $m_x \omega^2 \ell^2 / EA$
G,H = transformed stiffness matrices
GJ = torsional stiffness of member
h^2 = $m_x \omega^2 \ell^2 / GJ$
I_j = area moment of inertia of member about x_j axis
J = joint mass matrix
K = global stiffness matrix
ℓ = length of member
m_x = mass per unit length of member where x is $a,c,d,$ or r
M_j = moment on end of member about x_j axis
n = circumferential wave number
n_s = number of axial or ring members
P = axial load on column
P_j = load on end of member in x_j direction
P_0 = axial load in member due to pretension
P_x = member preload where x is $a,c,d,$ or r
Q = radial load
r = radius of cylinder
R,S = stiffness matrices for member in local coordinates
t = shell wall thickness
u_j = displacement at end of member in x_j direction
U_j = displacement vector for node j [see Eq. (1)]
w = mass per unit area of shell wall
x = axial coordinate
x_j = local Cartesian coordinates for member
y_j^2 = $P_x \ell^2 / EI_j$
z_j^4 = $m_x \omega^2 \ell^4 / EI_j$
α = π / n_s
θ = angle between diagonal and axial members
λ = longitudinal half-wavelength
ν = Poisson's ratio
ρ = radius of gyration
ϕ = circumferential coordinate
ψ = rotation at end of member about x_j axis
ω = $2\pi f$, circular frequency

Subscripts

a = axial member
c = cable member
d = diagonal member
r = ring member
(If subscript is not used, all members are identical)
$1,2,3$ = x_1, x_2, x_3 direction for local member properties, loadings, and displacements
j = node j or a member connecting node 0 to node j

Introduction

LATTICE structures of the type shown in Fig. 1 and cable-stiffened ring structures of the type shown in Fig. 2 are often proposed for very large space structures. To simplify erection and/or deployment, such structural systems usually consist of repetitive arrays involving only a few different types of members; however, these structural systems may involve thousands of structural nodes. Dynamic characteristics of these structures are an important design consideration. Simple and accurate analysis methods not requiring complete modeling of the structure will certainly be desirable or, in some cases, mandatory. The purpose of this paper is to present such an analysis for vibration of a certain family of lattice structures shown in Fig. 3. The repetitive nature of these configurations was used by Anderson[1] to develop a buckling analysis for these same configurations. In the present paper, this analysis is extended to include vibration with the effects of initial stress. The analysis is exact for the lattice beam with simply supported ends and for the ring configuration assuming a rigid central mast. The solution is also reasonably accurate for vibration modes with short axial wavelengths that are not greatly affected by boundary conditions. All of the vibration frequencies can be obtained from the eigenvalues of a 6×6 matrix.

Configurations

The configurations analyzed are shown in Fig. 3. The double-laced truss may have any number of longitudinal members greater than one. The configuration shown, the three-element beam, is a common form of this general structure. Circumferential or ring members may also be

Presented as Paper 81-0620 at the AIAA Dynamics Specialists Conference, Atlanta, Ga., April 9-10, 1981; submitted April 24, 1981; revision received Aug. 24, 1981. This paper is declared a work of the U.S. Government and therefore is in the public domain.

*Principal Scientist, Structural Concepts Branch, Structures and Dynamics Division. Associate Fellow AIAA.

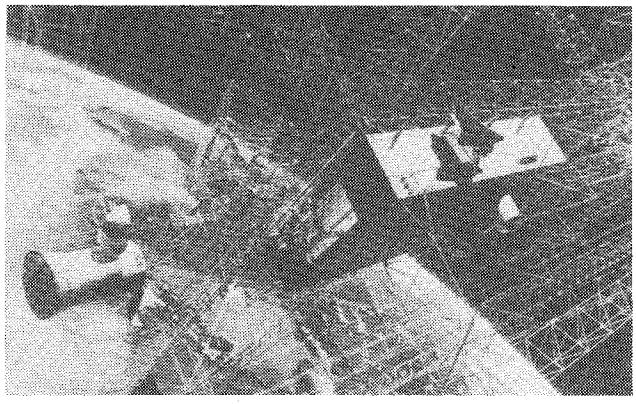

Fig. 1 Lattice structures for space application.

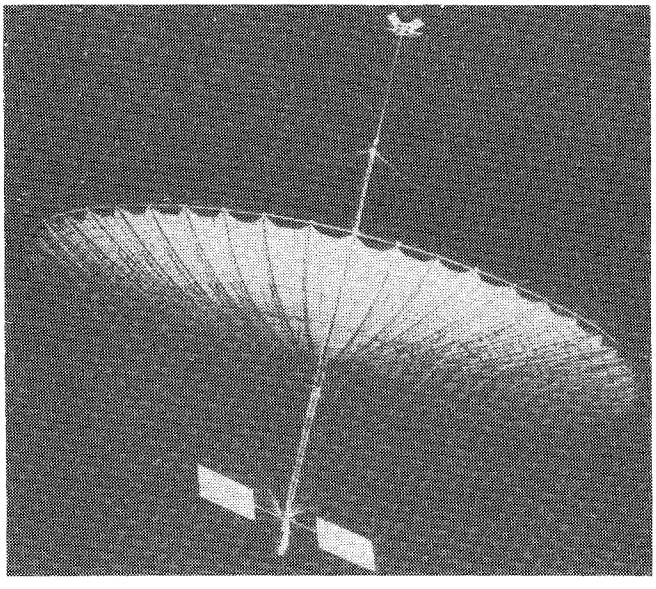

Fig. 2 Cable-stiffened ring supporting antenna surface.

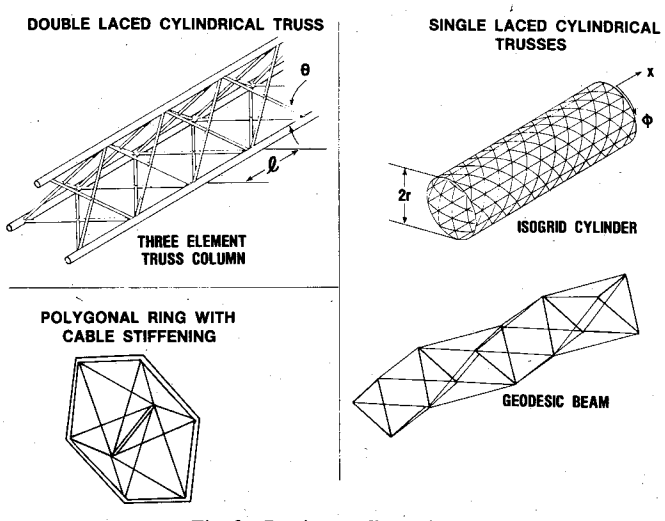

Fig. 3 Lattice configurations.

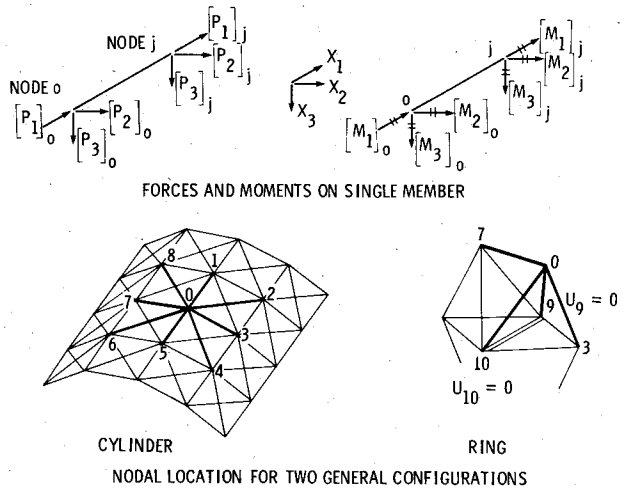

Fig. 4 Member loads and geometry.

present. It is assumed that the diagonal members are not joined at the points where they cross. Thus, the only structural nodes are on the longitudinal members.

The single-laced configurations have two possible arrangements—one with axial members and one with circumferential or ring members. There must be an even number of axial members for geometric compatibility, but there may be any number of ring members greater than one. The isogrid cylinder is shown as an example of a single-laced truss with axial members. The configuration shown with three members making up a ring is typically denoted a "geodesic beam."

The final configuration shown in Fig. 3 is a polygonal ring that may have a central mast with tension cables connected to each vertex of the ring. The mast is assumed rigid so that its displacements are zero. Thus the only structural nodes that enter the analysis are on the ring.

The cylindrical configurations may be loaded by an axial load. If both ring and diagonal members are present, the double-laced configuration may have an internal self-equilibrating force system. The ring may have external radial loads at each vertex plus an internal self-equilibrating force system due to tension in the cable stiffening.

Method of Analysis

For the configurations of Fig. 3 and the assumptions of the previous section, the analyzed structures are periodic such that every internal structural node is connected to its neighbor in exactly the same geometric pattern. The analysis starts with the relation between forces, moments, displacements, and rotations at the end of a single member. If a member connects node 0 to node j along the x_1 axis, the forces and moments (see Fig. 4a) at node 0 are:

$$F_0 = RU_0 + SU_j \tag{1}$$

where

$$F_i^T = [P_1, P_2, P_3, M_1, M_2, M_3]_i$$

$$U_i^T = [u_1, u_2, u_3, \psi_1, \psi_2, \psi_3]_i$$

The two 6×6 matrices, R and S, are similar to the upper half of the usual finite-element stiffness matrix, except that the linear stiffness terms are multiplied by dynamic stiffness coefficients developed by Howson[2] to account for the effects of axial load and frequency. Because these coefficients are developed from the exact solution of the beam-differential equation, the exact behavior for all vibration modes is represented without requiring intervening nodes. The matrices R and S are given in the Appendix.

Conventional finite-element transformation matrices are used to write the equilibrium equations at a node in terms of the displacement of a typical node and the displacements of adjacent nodes. These equations are as follows:

$$\sum_j (G_j U_0 + H_j U_j) = \omega^2 J U_0 \tag{2}$$

The matrices G_j and H_j are obtained by transforming R and S from the local element coordinate system to global cylindrical coordinates. The mass matrix J includes only the effect of concentrated masses at the nodes; member mass is included in the matrices G and H. The joint mass matrix is given in the Appendix. The summation is over all members at a node as illustrated in Fig. 4b. Because the structure is periodic, a simple trigonometric mode shape satisfies the equilibrium equations. The following expression is taken for U:

$$U = U_0 e^{i\pi x/\lambda} e^{in\phi} \tag{3}$$

where x is the axial coordinate and ϕ the circumferential coordinate. The resulting mode shape has n circumferential waves and an axial half-wavelength λ with boundary conditions of simple support at this spacing. Equation (3) can be used to eliminate the displacements at the adjacent nodes in Eq. (2), which can then be written as

$$(K - \omega^2 J) U_0 = 0 \tag{4}$$

where K is the assembled global stiffness matrix given by Anderson.[1]

The method of solution is similar to Bleich[3] who developed a difference equation similar to Eq. (2) for buckling of a planar frame with repetitive geometry. The general solution to Eq. (2) would be quite difficult, with Eq. (3) being just one possibility. There is, of course, no control over boundary conditions, but examination of the solution shows that the classical simple support condition is satisfied at the ends of the cylindrical configurations.

Results

There are an infinity of eigenvalues contained in the 6×6 matrix from Eq. (4) for each combination of λ and n because of the transcendental character of the stiffness matrix. The method presented by Wittrick[4] was used to find desired eigenvalues. In this method, the matrix is converted to upper triangular form by a process of Gaussian elimination. The number of negative terms on the diagonal is called the sign count of the matrix. The sign count plus the number of clamped member frequencies exceeded is the total number of eigenvalues exceeded for the trial value of frequency. A simple iterative process allows convergence to any desired accuracy. Instead of carrying this method to complete convergence, whenever a particular eigenvalue was isolated between upper and lower bounds, the method given by Thurston[5] was used to obtain final convergence. This method is a Newton method that exhibits quadratic convergence. Results were obtained for vibration of a number of configurations and are discussed in the following sections.

Isogrid Cylinder

A lattice configuration consisting of members oriented at 0 ± 60 deg has isotropic properties and is commonly termed an "isogrid" array. If an isogrid array is formed into a circular cylinder, it should behave similar to an equivalent isotropic shell assuming member size is small compared to cylinder radius. A study was made of the vibration characteristics of an isogrid cylinder modeled as a lattice structure. Results from the lattice analysis were compared with results from shell theory. The stiffness and mass of the shell is the same as the isogrid for the following set of properties:

$$t = \sqrt{12}\rho \qquad E_s = EA/3\rho\ell \qquad \nu = 1/3 \qquad w = 2\sqrt{3}m/\ell \tag{5}$$

The radius of the cylinder is

$$r = \frac{\sqrt{3}\ell}{4\sin\alpha} \approx \frac{\sqrt{3}\ell n_s}{4\pi} \tag{6}$$

The radius-to-thickness ratio is then

$$\frac{r}{t} = \frac{\ell}{\rho}\frac{n_s}{8\pi} \tag{7}$$

Frequencies of two simply supported isogrid cylinders with an equivalent shell r/t of 150 are shown in Fig. 5 along with results from Sanders shell theory obtained by Cooper.[6] The first three modes for an axial half-wavelength equal to three times the shell radius are shown as a function of circumferential harmonic number n. The lowest curve corresponds to a flexural mode except at $n=0$ where the lowest point is the first torsion mode. The upper curves are predominantly in-plane modes. Equation (7) shows that if the product $(\ell/\rho)n_s$ is constant, then the equivalent r/t is constant. For small ℓ/ρ and large n_s the results for the lattice analysis tend to agree with shell theory. For large ℓ/ρ and small n_s, on the other hand, there is disagreement between lattice analysis and shell theory for the higher modes. The trend for lattice structures with large ℓ/ρ and small n_s to deviate from predictions of shell theory was also found for buckling by Anderson.[1]

Three-Element Truss Column

Mikulas[7] studied optimum proportions of three-element truss columns for carrying axial loading. Vibration characteristics of a particular column from this study are shown in Fig. 6. The column is 50 m long and is designed to carry an axial load of 5000 N. It is fabricated from graphite-epoxy. Frequency at zero axial load is plotted for different axial wave numbers. To compare the results from the lattice analysis with those from beam theory, equivalent bending, transverse shear, and torsional stiffnesses are calculated for

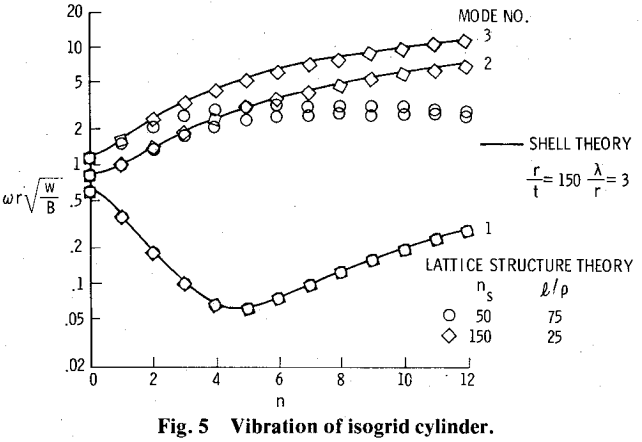

Fig. 5 Vibration of isogrid cylinder.

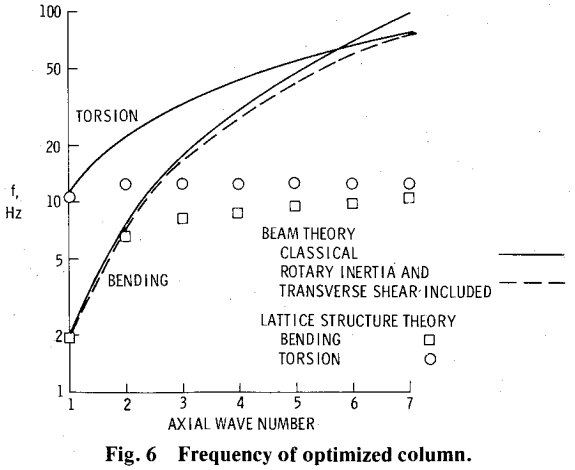

Fig. 6 Frequency of optimized column.

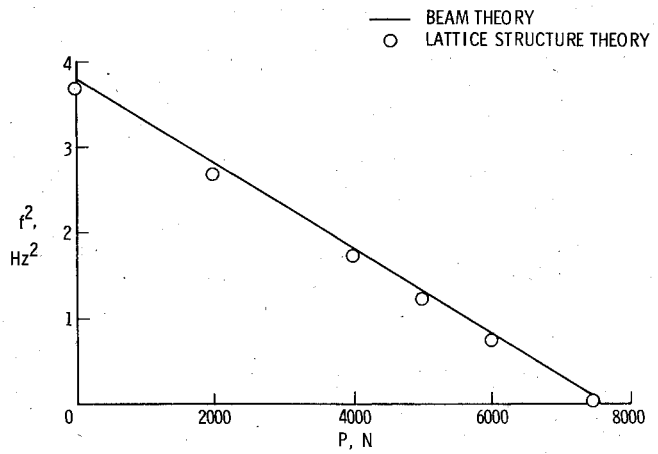

Fig. 7 Effect of axial load on fundamental bending frequency of three-element column.

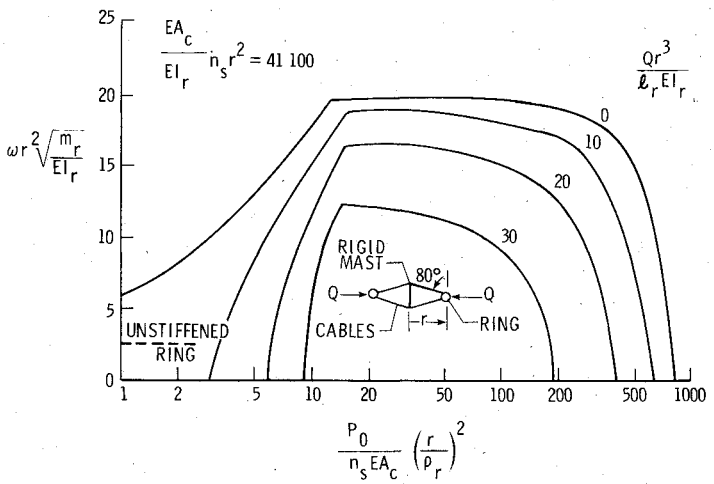

Fig. 8 Vibration of prestressed cable-stiffened ring.

the truss column. For bending vibrations, both classical and Timoshenko[8] beam theory results are given. The square symbols are from the lattice analysis with $n=1$ corresponding to a bending mode; the circle symbols are for $n=0$, which is a torsion mode. The fundamental bending and torsion modes show good agreement between beam theory and the lattice analysis. For all the higher torsion modes and the bending modes beyond the second, the lattice analysis gives results considerably below those from beam theory. The reason for this result is that the clamped-end frequency of the diagonal members is 12.3 Hz, which becomes an upper limit for the lowest frequency for each n number.

The effect of axial load on the fundamental bending frequency of the three-element truss column is shown in Fig. 7. Results from beam theory predict a linear relation between frequency squared and load shown by the straight line on the figure. The results from the lattice analysis also tend to fall on a straight line slightly below the beam theory results. The load at zero frequency is the buckling load corresponding to the Euler column value. It is about 50% greater than the column design load to allow for imperfections that were assumed as design requirements by Mikulas.[7]

Cable-Stiffened Ring

The antenna concept shown in Fig. 2 has been idealized structurally to the cable-stiffened polygonal ring shown in Fig. 3. The central mast is assumed to be sufficiently stiff that its deformations may be neglected. The antenna surface is stretched in the interior of the ring to produce an inward radial load Q acting at discrete points around the circumference. The pretensioned cables also produce a radial load that produces compression in the ring. Anderson[1] studied the buckling characteristics of such a ring as a function of pretension load. Vibration characteristics of the same cable-stiffened ring are shown in Fig. 8. A dimensionless frequency parameter is plotted as a function of a pretension parameter for selected values of the radial force Q. The mass of the antenna surface is not included. Results are shown for ring modes ($n \geq 2$) for which the deflection of the mast must be zero without any assumption. Each curve for nonzero Q starts at a value of pretension that is just sufficient to prevent the cables from being slack. The frequency then increases from zero corresponding to the cable vibration mode. Further increases in pretension cause the out-of-plane ring modes to become lower than the cable frequency. The critical circumferential wave number increases with pretension until it reaches five, which is the critical harmonic for buckling. The curves rapidly approach zero as combination of the radial force Q and the cable tension produce a compressive force in the ring that causes buckling. The two zero-frequency points for each curve agree with the buckling values reported by Anderson.[1]

Concluding Remarks

A simple but accurate theory is developed for vibration of a general class of lattice structures having repetitive geometry. For beamlike lattice structures, the solution is exact for simply supported ends. The effect of initial stress in the members is included. Studies of an isogrid cylinder and a three-element truss column show that local member vibration can reduce the frequency from that predicted from idealization of the structure as an equivalent shell or beam. This effect is especially important for higher modes. The effect of axial load on the fundamental bending frequency of a three-element truss column is shown to be essentially the same as predicted by beam theory. Deviations from beam or shell theory models of the structures studied are greatest for structures with a small number of slender members. Study of a cable-stiffened ring shows the different regimes of cable pretension where buckling occurs, where the lowest vibration mode is dominated by motion of the cables, and where the lowest mode is dominated by motion of the ring. At certain values of pretension, vibration frequencies are considerably increased over that of an unstiffened ring.

Appendix

Member Stiffness Matrix

The analysis presented in the main part of the paper is based on the exact representation of the stiffness of an individual beam member when loaded by an axial load and undergoing harmonic vibration. The stiffness matrix has the form of the usual finite-element stiffness matrix, but the individual terms are modified by the dynamic stiffness coefficients of Howson.[2] The two matrices required in the analysis are as follows:

$$R = \begin{bmatrix} R_{11} & 0 & 0 & 0 & 0 & 0 \\ & R_{22} & 0 & 0 & 0 & R_{26} \\ & & R_{33} & 0 & R_{35} & 0 \\ & & & R_{44} & 0 & 0 \\ & \text{SYM} & & & R_{55} & 0 \\ & & & & & R_{66} \end{bmatrix} \tag{A1}$$

$$S=\begin{bmatrix} S_{11} & 0 & 0 & 0 & 0 & 0 \\ 0 & S_{22} & 0 & 0 & 0 & S_{26} \\ 0 & 0 & S_{33} & 0 & S_{35} & 0 \\ 0 & 0 & 0 & S_{44} & 0 & 0 \\ 0 & 0 & -S_{35} & & S_{55} & 0 \\ 0 & -S_{26} & 0 & 0 & 0 & S_{66} \end{bmatrix} \tag{A2}$$

where:

$$R_{11}=f_7EA/\ell \qquad S_{11}=-f_8EA/\ell$$

$$R_{22}=12f_{43}EI_3/\ell^3 \qquad S_{22}=-12f_{53}EI_3/\ell^3$$

$$R_{26}=6f_{33}EI_3/\ell^2 \qquad S_{26}=6f_{63}EI_3/\ell^2$$

$$R_{33}=12f_{42}EI_2/\ell^3 \qquad S_{33}=-12f_{52}EI_2/\ell^3$$

$$R_{35}=-6f_{32}EI_2/\ell^2 \qquad S_{35}=-6f_{62}EI_2/\ell^2$$

$$R_{44}=f_9GJ/\ell \qquad S_{44}=f_{10}GJ/\ell$$

$$R_{55}=4f_{12}EI_2/\ell \qquad S_{55}=2f_{22}EI_2/\ell$$

$$R_{66}=4f_{13}EI_3/\ell \qquad S_{66}=2f_{23}EI_3/\ell$$

$$f_{1j}=(d_j^2+2e_j^2)[\cosh(d_j)\sin(e_j)/e_j-\sinh(d_j)\cos(e_j)/d_j]/8\Delta_j$$

$$f_{2j}=(d_j^2+e_j^2)[\sinh(d_j)/d_j-\sin(e_j)/e_j]/4\Delta_j$$

$$f_{3j}=[(d_j^2-e_j^2)(\cosh(d_j)\cos(e_j)-1)+2d_je_j\sinh(d_j)\sin(e_j)]/12\Delta_j$$

$$f_{4j}=(d_j^2+e_j^2)[e_j\cosh(d_j)\sin(e_j)+d_j\sinh(d_j)\cos(e_j)]/24\Delta_j$$

$$f_{5j}=(d_j^2+e_j^2)[e_j\sin(e_j)+d_j\sinh(d_j)]/24\Delta_j$$

$$f_{6j}=(d_j^2+e_j^2)[\cosh(d_j)-\cos(e_j)]/12\Delta_j$$

$$f_7=g\cot g \qquad f_8=g\csc g \qquad f_9=h\coth \qquad f_{10}=h\operatorname{csch}$$

$$\Delta_j=1-\cosh(d_j)\cos(e_j)+(d_j^2-e_j^2)\sinh(d_j)\sin(e_j)/(2d_je_j)$$

$$d_j^2=[-y_j^2+(y_j^4+4z_j^2)^{1/2}]/2$$

$$e_j^2=[y_j^2+(y_j^4+4z_j^2)^{1/2}]/2$$

$$y_j^2=P_x\ell^2/EI_j \qquad z_j^4=m_x\omega^2\ell^4/EI_j$$

$$g^2=m_x\omega^2\ell^2/EA \qquad h^2=m_x\omega^2\ell^2/GJ$$

$$\lim_{\substack{y_j\to 0\\ z_j\to 0}} f_{ij}=1 \tag{A3}$$

The coefficients f_{ij} and g can be obtained from Howson[2] by letting the transverse shear and rotary inertia terms go to zero. The differential equation for torsional vibration is identical in form to the equation for axial vibration. Thus the stiffness terms for torsion are of the same form as for axial vibration.

The global stiffness matrices used in Eq. (2) are obtained from the usual finite-element transformations as follows:

$$G=T^TRT \qquad H=T^TST' \tag{A4}$$

where:

$$T=\begin{bmatrix} W & 0 \\ 0 & W \end{bmatrix} \qquad W=\begin{bmatrix} c_\beta & s_\beta c_\epsilon & s_\beta s_\epsilon \\ -s_\beta & c_\beta c_\epsilon & c_\beta s_\epsilon \\ 0 & -s_\epsilon & c_\epsilon \end{bmatrix} \tag{A5}$$

$$T'(\beta,\epsilon)=T(\beta,-\epsilon)$$

The subscripts in Eq. (A5) were omitted in Ref. 1; therefore, the equation is included here for completeness. Values for β and ϵ are given in the reference.

The dynamic stiffness coefficients properly account for the distributed member mass. If a concentrated mass is present at a node such as a joint or fitting, its effect may be included through the joint mass matrix given as follows:

$$J=\operatorname{diag}[C,C,C,C_1,C_2,C_3] \tag{A6}$$

References

[1] Anderson, M. S., "Buckling of Periodic Lattice Structures," *AIAA Journal*, Vol. 19, June 1981, pp. 782-788.

[2] Howson, W. P. and Williams, F. W., "Natural Frequencies of Frames with Axially Loaded Timoshenko Members," *Journal of Sound and Vibration*, Vol. 26, No. 4, 1973, pp. 503-515.

[3] Bleich, F., *Buckling Strength of Metal Structures*, 1st ed., McGraw-Hill Book Co. Inc., New York, 1952, pp. 260-267.

[4] Wittrick, W. H. and Williams, F. W., "A General Algorithm for Computing Natural Frequencies of Elastic Structures," *Quarterly Journal of Mechanics and Applied Mathematics*, Vol. 14, Pt. 3, Aug. 1971, pp. 263-284.

[5] Thurston, G. A., "Roots of Lambda Matrices," *Journal of Applied Mechanics*, Vol. 45, No. 4, Dec. 1978, pp. 859-863.

[6] Cooper, P. A., "Vibration and Buckling of Prestressed Shells of Revolution," NASA TN D-3831, March 1967.

[7] Mikulas, M. M., "Structural Efficiency of Long Lightly Loaded Truss and Isogrid Columns for Space Application," NASA TM 78687, July 1978.

[8] Timoshenko, S., *Vibration Problems in Engineering*, 2nd ed., D. Van Nostrand Co. Inc., 1937, pp. 341-342.